IMPROVEMENT OF MIXING VANE CROSSFLOW MODEL IN SUBCHANNEL ANALYSIS

Hu Mao, Bao-Wen Yang*, Jianqiang Shan, Bo Zhang
Science and Technology Center for Advanced Fuel Research & Development, School of Nuclear Science and Technology, Xi'an Jiaotong University
Xianning West Rd. 28, Xi'an, Shaanxi 710049, P.R. China
*bwy@mail.xjtu.edu.cn

ABSTRACT

Subchannel analysis is widely used for development of CHF correlations and prediction of CHF values and locations; however, the current subchannel codes usually neither reflect the contribution of spacer grid mixing vanes on local crossflow, nor do they present the difference between various types of mixing vanes and their influence on flow field. The lack of crossflow modeling leads to major challenge on predicting CHF values and CHF locations in an axially non-uniform heating system, such as the reactor core. In a high axial power peaking system, not only the prediction of CHF value, but also the prediction of CHF location are critical in properly providing safety margin. Therefore, it is necessary to improve the mixing vane crossflow model in subchannel analysis. This paper presents the improvement of mixing vane crossflow model by applying the Distributed Resistance Method (DRM). The term of mixing vane resistance is expressed in momentum equations of subchannel analysis, and the new equations are solved to obtain the influence of mixing vanes on local pressure drop and crossflow. The improved (with DRM) model is applied to subchannel code COBRA-Ⅳ to analyze thermal hydraulic performance in a 5x5 rod bundle with one spacer grid having classical split vanes. The results are compared with those of numerical analysis available in literature. The results show that mixing vanes not only cause increase of local pressure drop in subchannels, but also cause increase of local crossflow in gaps among fuel rods, which reduces modeling uncertainties in lumped parameter codes. The analysis indicates that the improved mixing vane crossflow model performs satisfactorily predicting the most important qualitative trends for flows in rod bundle with spacer grid having mixing vanes, therefore it could be used as an approach to optimize the parametric studies for grid design.

KEYWORDS
Crossflow, mixing vane, distributed resistance method, subchannel analysis

1. INTRODUCTION

Subchannel analysis is widely used for reactor core thermal hydraulic calculation and safety analysis. Development of CHF correlations for accurate prediction of CHF values and locations is an important task for reactor core safety analysis. One of the key factors in obtaining reliable CHF values and locations prediction is to accurately estimate rod bundle local parameter conditions. Spacer grid has great effect on rod bundle local flow field and local parameters, and spacer grid with mixing vanes especially contributes to the change of local pressure drop in subchannels and local crossflow in the gaps. Rowe [1] proposed forced crossflow model which distributes a certain percentage of each subchannel's axial flow to adjacent gaps. The forced crossflow model is applied to COBRA-IIIC. Because the percentage values of axial flow across the gaps are completely empirical, the calculation results have a relatively large range of

uncertainties. In the later version of COBRA series codes, F-COBRA-TF, the influence of spacer grid on local flow field is considered by applying the spacer pressure loss coefficient [2]. For each geometrical subchannel type, an individual spacer pressure loss coefficient is needed as an input value for F-COBRA-TF calculation.

However, the values of the individual spacer pressure loss coefficients in F-COBRA-TF depend on experimental results and are difficult to generalize to rod bundle with different shapes and sizes of spacer grids. Besides, the individual spacer pressure loss coefficients only reflect the pressure loss caused by the mixing vane grid on the axial direction, and they don't reflect the contribution of spacer grid mixing vanes on local crossflow between neighboring subchannels or fuel rod gaps. They cannot accurately reflect the contribution of spacer grid mixing vanes on local crossflow. This will cause a relative large range of uncertainties in local parameters prediction, leading to deviations of CHF values and CHF locations prediction. Therefore, it is necessary to improve the mixing vane crossflow model to reflect the contribution of spacer grid mixing vanes on local pressure drop and crossflow, which are essential to rod bundle local parameter conditions and CHF prediction.

This paper applies the Distributed Resistance Method (DRM) [3] to improve mixing vane crossflow model. The effects of mixing vanes are considered by adding mixing vane resistance in the momentum equations of subchannel code COBRA-Ⅳ. The new equations are solved employing Gauss-Seidel iteration method. The thermal hydraulic performance in a 5x5 rod bundle with one spacer grid having classical split vanes is then calculated applying the improved (with DRM) model. Local pressure drop and crossflow are analyzed and the capacity of the improved model is preliminarily evaluated.

2. MIXING VANE CROSSFLOW MODEL

Since the Distributed Resistance Method (DRM) could account for the radially diversion of momentum resulting from the presence of mixing vane and reduce modeling uncertainties in lumped parameter codes, the DRM is applied to improve the mixing vane crossflow model. The improvement is based on the following assumptions:

(a) The friction force along the "parallel" directions can be estimated by projecting the friction force along the velocity direction in these parallel directions.
(b) The friction force along any direction can be estimated using Rehme's friction factor correlations [4,5].
(c) The total friction force is uniformly distributed among the mixing vane surfaces.
(d) Rod bundle axial direction parallels to vertical direction.
(e) Axial flow predominates in flow field.

On the basis of the above assumptions, the mixing vane crossflow model is described as follows.

Firstly, the local velocity in the subchannel is defined as V_{total}, and the angle between the rod axial direction and the local velocity is recorded as θ, as shown in Figure 1(a). The local velocity V_{total} is decomposed into rod axial and lateral directions, and the rod axial component u and the rod lateral component v can be obtained; again the local velocity V_{total} is decomposed into mixing vane tangential and normal directions, and the mixing vane tangential component u_1 and the mixing vane normal component v_1 can be obtained. θ is the function of u_1 and v_1, and it is solved together with u_1 and v_1 by iteration.

Secondly, based on the assumption (a) , the Rehme's correlation [4,5] and the Gunter-Shaw correlation [6] are used to express the component of force F_u, F_v, F_{u1} and F_{v1}, which correspond to four components of the velocity V_{total}, namely, u, v, u_1 and v_1, respectively, as shown in Figure 1(b).

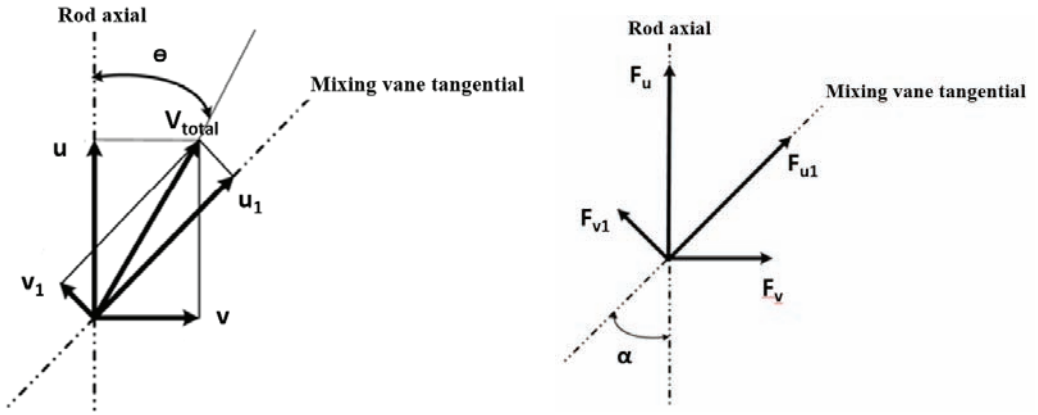

(a) (b)

Figure 1. Schematic diagram of the Distributed Resistance Method

A detailed expressions are listed below.
Rehme's correlation:

$$R(V_{total}) = \frac{A_W'' f_M (V_{total})}{8} \rho V_{total}^{\ 2} \tag{1}$$

Gunter-Shaw correlation:

$$G_v = \frac{A_W'' f_G}{8} \rho v^2 (\frac{D_V''}{P})^{0.4} \tag{2}$$

Expressions of the component forces:

$$F_{\mathrm{u}} = R(V_{total})(\frac{A_R}{A_W''}) \cos\theta \tag{3}$$

$$\mathrm{F}_{u1} = R(V_{total})(1-\frac{A_R}{A_W''}) \cos(\alpha-\theta) \tag{4}$$

$$\mathrm{F}_v = \frac{A_W'' f_G}{8} \rho v^2 (\frac{D_V''}{P})^{0.4} \tag{5}$$

$$\mathrm{F}_{v1} = \frac{A f_n}{2} \rho v_1^{\ 2} \tag{6}$$

where f_M is the single-phase flow friction coefficient; A_W'' is the total wetted solid surface area of the subchannel including the mixing vane.

$$A_W'' = A_R + A_W \tag{7}$$

$$\theta = \arctan\left(\frac{\mathrm{v}_1}{\mathrm{u}_1}\right) \tag{8}$$

Where A_R is the wetted solid surface area of the subchannel excluding the mixing vane, and A_W is the mixing vane's wetted solid surface area. D_V'' is the equivalent hydraulic diameter including the mixing vane, and P is the rod-to-rod pitch. α is the angle between the rod axial direction and mixing vane's tangential direction, as shown in Figure 1.

$$f_G = \begin{cases} 180/\mathrm{Re}_{Dv} & laminar\ \ flow \\ 1.92/\mathrm{Re}_{Dv}^{0.145} & turbulent\ flow \end{cases} \tag{9}$$

where $\mathrm{Re}_{Dv} = \dfrac{\rho D_V u_g}{\mu}$, u_g is the crossflow velocity across the gap, and D_V is the equivalent hydraulic diameter without the mixing vane.

$$f_n = C_0 \left(\frac{A_g}{A_{mg}} \right)^n \left[1 + \frac{C_1}{\mathrm{Re}^m} \right] \tag{10}$$

where A_g is the gap flow area without mixing vane, and A_{mg} is the gap flow area with mixing vane; C_0, C_1, m and n are constant parameters. All the forces are expressed as functions of rod bundle geometry and local velocity.

Thirdly, the tangential component F_{u1} and the normal component F_{v1} are decomposed into rod axial and lateral directions, and the expressions of total axial force and total lateral force are obtained.
Total axial force:

$$F_A = F_u + F_{u1}\cos\alpha + F_{v1}\sin\alpha \tag{11}$$

Total lateral force:

$$F_L = F_v + F_{u1}\sin\alpha - F_{v1}\cos\alpha \tag{12}$$

Finally, total axial force and total lateral force are added to the axial and transverse momentum equations of subchannel code COBRA-Ⅳ respectively.
Axial momentum equation:

$$\begin{aligned} &\frac{\partial}{\partial t} << \rho u >>_V A + \frac{\partial}{\partial X} < \rho u^2 >_A A + [D_c^T] < \rho u v >_S S \\ &= -A\frac{\partial}{\partial X} < p >_A - \frac{\partial}{\partial X}\left(F_u + F_{u1}\cos\alpha + F_{v1}\sin\alpha \right) \\ &\quad - Ag << \rho >>_V - C_T [D_c^T]\{W'\}[D_C]\{u'\} \end{aligned} \tag{13}$$

Transverse momentum equation:

$$\begin{aligned} &\frac{\partial}{\partial t} << \rho v >>_{V'} S + \frac{\partial}{\partial X} < \rho v u >_{A'} S + C_S [D_C][D_c^T]\left\{ (N)\frac{S}{\ell} < \rho v^2 >_S \cos\Delta\beta \right\} \\ &= -\frac{1}{\ell}\frac{\partial}{\partial X}\left(F_v + F_{u1}\sin\alpha - F_{v1}\cos\alpha \right) + \frac{S}{\ell}[D_C]\{< p >_A\} - << \rho >>_{V'} S\cos\beta \end{aligned} \tag{14}$$

The new equations are solved employing Gauss-Seidel iteration method, and the effect of mixing vanes on local flow field can be obtained.

3. CALCULATION AND ANALYSIS

3.1. Calculation Conditions

The thermal hydraulics performance of a 5x5 rod bundle with one spacer grid having classical split vanes is calculated, using subchannel code COBRA-Ⅳ applying the improved (with DRM) model. The spacer grid with mixing vanes is located at 105 mm above the bottom of the rod bundle, as shown in Figure 2. The flow field of the 5x5 rod bundle is divided into 36 subchannels. The mixing vanes arrangement and subchannel numbers are shown in Figure 3. Since lack of complete experiment data, this paper chose to compare the subchannel calculation results with CFD simulation results. For the purpose of comparative

analysis, the same calculation conditions as those of M.A. Navarro et al.'s numerical analysis of 5x5 rod bundle thermal hydraulic performance [7] is selected, and a detailed description of calculation conditions is listed in Table I. The number of axial node is set to 7 so as to allocate the spacer grid in a single control volume.

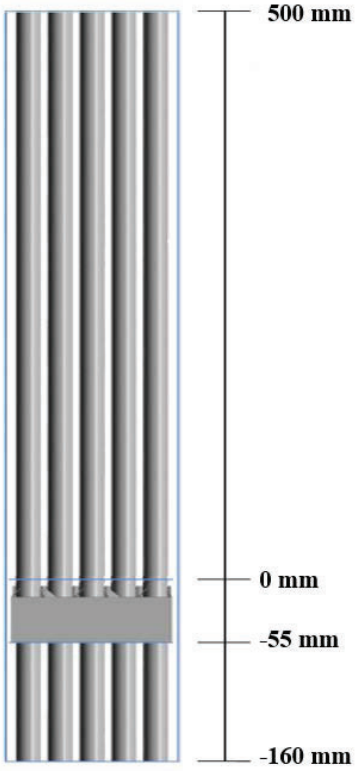

Figure2. The 5x5 rod bundle with one spacer grid having classical split vanes

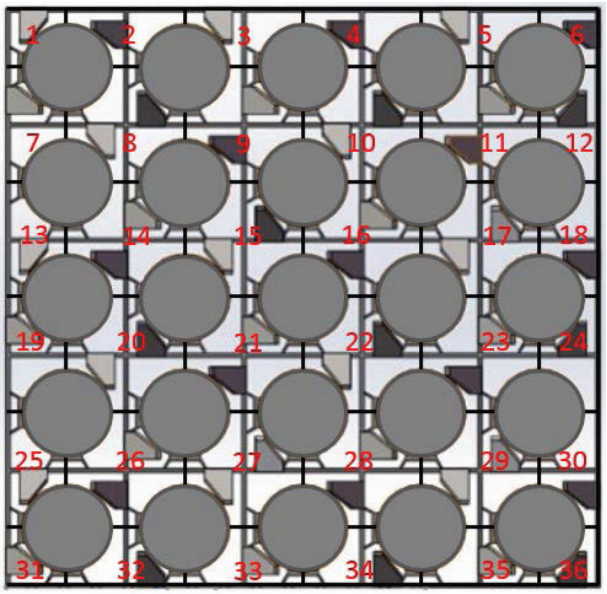

Figure 3. The subchannel numbers of the 5x5 rod bundle

Table I. Calculation conditions of 5x5 rod bundle with one spacer grid

Calculation parameters	Values
Rod bundle length	660mm
Rod diameter	9.5mm
Bundle pitch	12.6 mm
Hydraulic diameter (D_h)	11.21mm
Flow area	2851.95 mm^{-2}
Inlet temperature	300 ℃
Pressure	158 bar
Mass flux	2858 kg/m^2-s
Heat flux	0.707 MW/m^2

3.2. Calculation Results and Analysis

3.2.1. Pressure drop

To reflect the effect of mixing vanes on local pressure drop, both the average pressure drops with and without mixing vanes are calculated. The pressure at the outlet of the rod bundle is defined as 0 KPa, and the zero point of height is defined at 100 mm above the bottom of the rod bundle, as shown in Figure 4. The numerical calculation results of [7] are quoted in Figure 5 for comparative analysis. The results show that mixing vanes cause increase of local pressure drop. This is mainly due to the blockage of mixing vanes on the coolant flow area. Besides, the mixing vanes cause crossflow in gaps, which will contribute to more pressure loss as well.

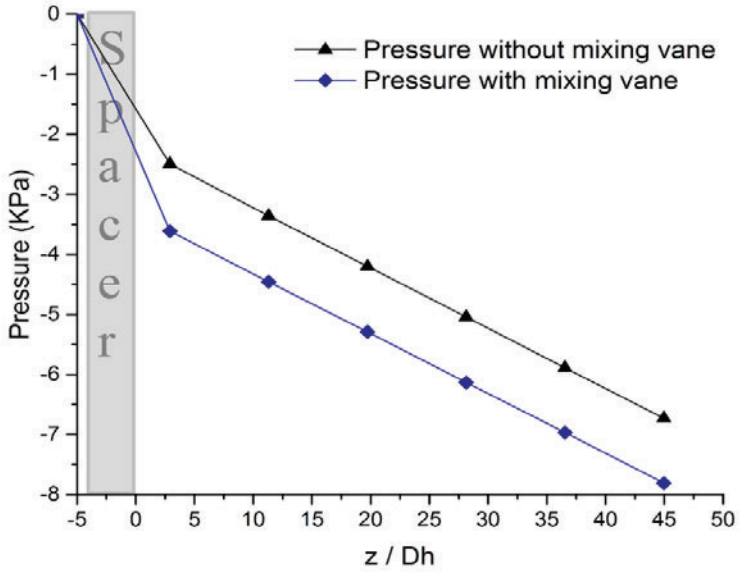

Figure 4. Pressure drops with and without mixing vanes in converted coordinates

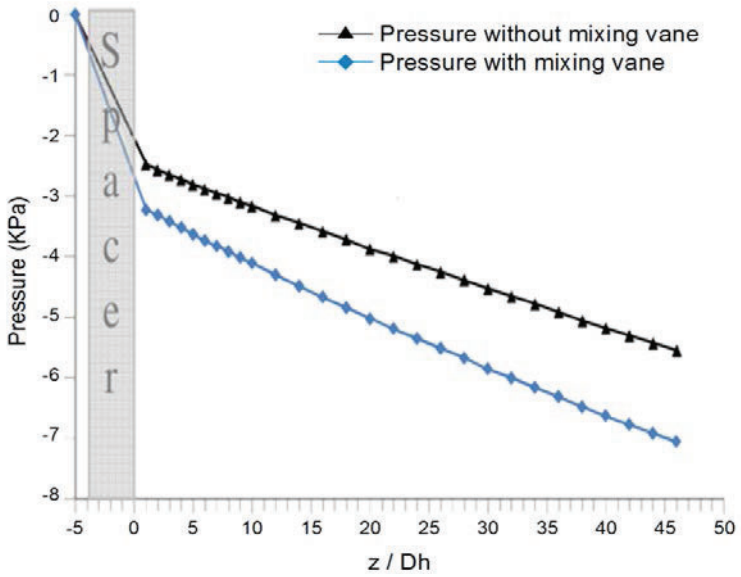

Figure 5. Pressure drops with and without mixing vanes of the numerical calculations [7]

Comparisons indicate that in subchannel calculation results the pressure difference between subchannels with and without mixing vanes is approximately constant along with the increase of height, which don't agree with the numerical calculation results using CFD code CFX 11.0. The reason should be that in CFX simulation, the eddy viscosity model $k-\varepsilon$ turbulence model that relates the turbulence kinetic energy k to the eddy dissipation ε was used, and the results contain combined influences of various types of mixing effect, including turbulent mixing as well as crossflow mixing caused by mixing vanes. While the conditions are simplified and a constant turbulent momentum factor (FTM) along with the length of the rod bundle is applied in COBRA-Ⅳ, which cannot accurately reflect the turbulent mixing effect, especially downstream of the spacer grid. Therefore, it is rather difficult to accurately reflect extra pressure drop caused by disordered flow field downstream of the spacer grid, so the turbulent mixing model in COBRA-Ⅳ need to be improved.

3.2.2. Crossflow

The calculation results of crossflow without and with the improved (with DRM) model are both presented, as shown in Figure 6 and 7. Both the results with and without the improved model show that the crossflow upstream of the spacer grid approximately equals to zero, and the crossflow increase in the spacer grid zone and decrease further downstream of the spacer grid. The distributions of crossflow in the 5x5 rod bundle are symmetrical corresponds to the geometrical symmetry. For example, the crossflow W(1,2) between subchannel 1 and 2 and the crossflow W(35,36) between subchannel 35 and 36 have approximately equal values and opposite signs, as shown in Figure 6 and 7, the same as W(2,8) and W(29,35), W(9,15) and W(22,28), etc.

When the improved model is not applied (shown in Figure 6), the peak crossflow is less than 1% of axial mass flux, much smaller than that with the improved model (nearly 6% of axial mass flux). The reason is that the crossflow without the improved model is caused by combined effect of spacer grid form loss and the geometric difference of subchannels (central, side and corner), which don't take into account the contribution of mixing vanes to crossflow. When the improved model is applied in the calculation, the mixing vanes effect on crossflow is fully considered.

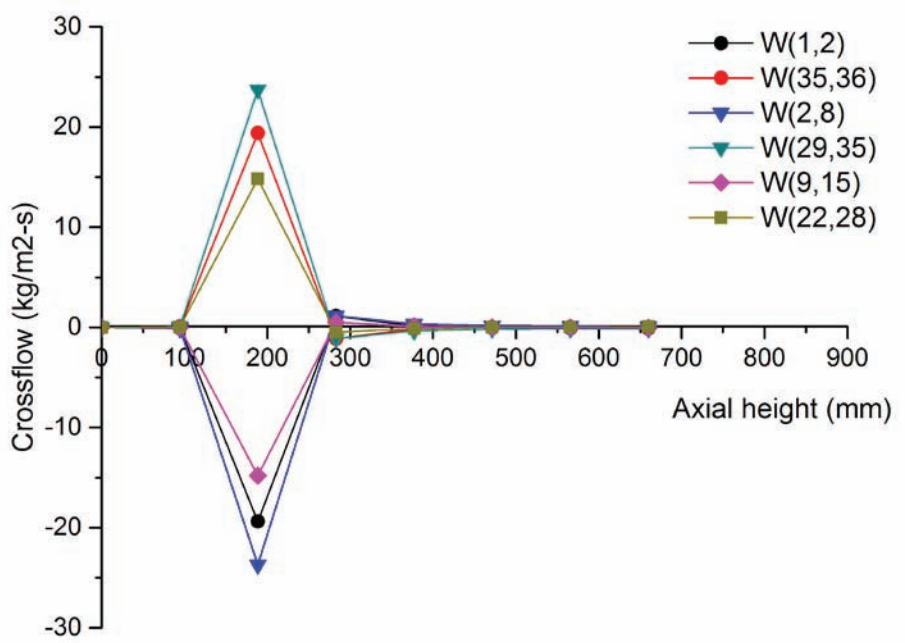

Figure 6. The crossflow in gaps in the symmetric positions without the improved model

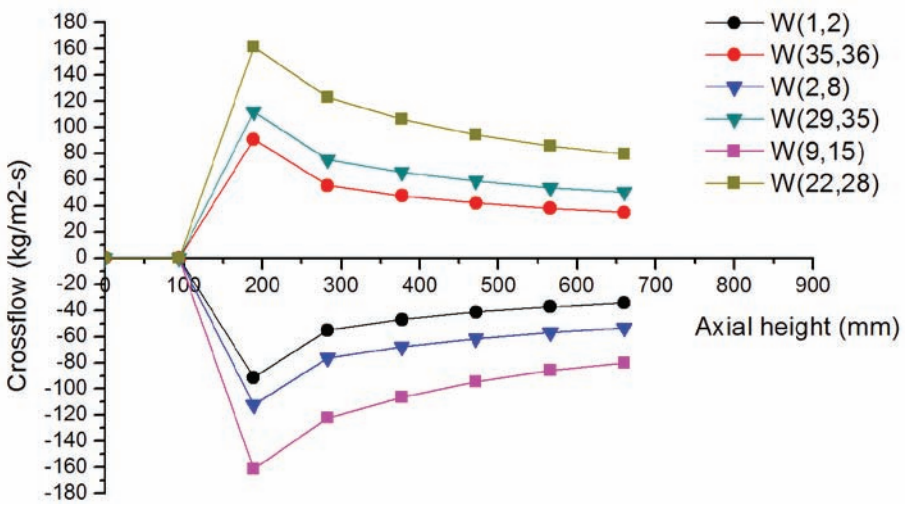

Figure 7. The crossflow in gaps in the symmetric positions with the improved model

The calculation results without the improved model show that crossflow downstream of the spacer grid decrease close zero sharply, as shown in Figure 6, which don't agree with numerical and experimental results available in literature [8-12]. Besides, the calculation results without the improved model don't predict qualitative flow trends correctly. When the improved model is applied, the direction trends of crossflow is in accordance with that of numerical and experimental analysis available in literature [8-12], and the results indicate that the improved (with DRM) model performed satisfactorily predicting the most important qualitative trends for flows in rod bundle with mixing vanes, as shown in Figure 8 [13].

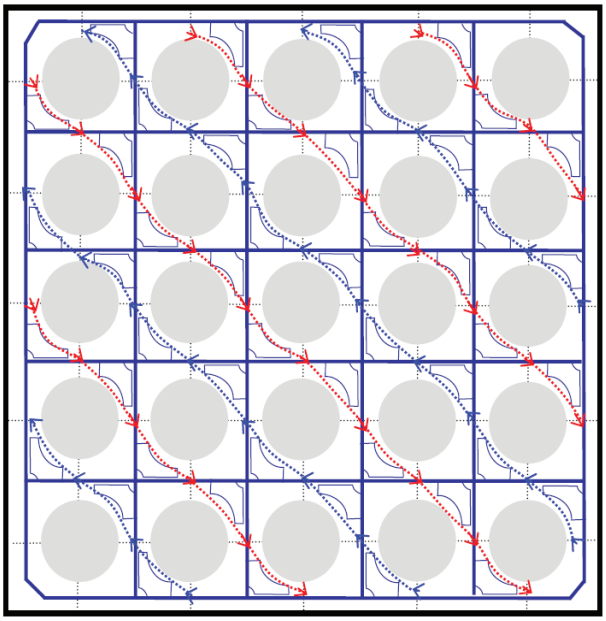

Figure 8. Meandering flow patterns in the 5x5 rod bundle with mixing vanes [13]

When the improved model is applied, the qualitative similarity of subchannel calculation results with numerical calculation results demonstrates that the improved model could be used as an approach to optimize the parametric studies for grid design.

4. CONCLUSIONS

This paper presents the improvement of mixing vane crossflow model. The Distributed Resistance Method (DRM) is applied to COBRA-Ⅳ and the term of mixing vane resistance is added to the momentum equations. By solving the new equations, the influence of mixing vanes on flow field is obtained. The improved (with DRM) model is applied for analysis of the thermal hydraulic performance in a 5x5 rod bundle with one spacer grid having classical split vanes. The local pressure drop and crossflow are compared with those of numerical analysis using CFD codes available in literature, and the capacity of the improved model is preliminarily evaluated.

The results show that mixing vanes cause increase of local pressure drop in subchannels and local crossflow between gaps. The increase of local pressure drop is mainly due to the blockage of mixing vanes on the coolant flow area as well as the disturbance of flow field downstream of the spacer grid. The distributions of crossflow in the 5x5 rod bundle are symmetrical corresponds to the geometric symmetry and the direction trends of crossflow is in accord with numerical analysis results available in literature.

The analysis indicates that the improved mixing vane crossflow model predicts the local pressure more accurately than without DRM, and performs satisfactorily predicting the most important qualitative trends for flows in rod bundle, so it could be used as an approach to optimize the parametric studies for grid design.

NOMENCLATURE

V_{total} local velocity in the subchannel

f_M	the single-phase flow friction coefficient
θ	the angle between the rod axial and the local velocity direction
α	the angle between the rod axial and the mixing vane's tangential direction
u	rod axial component of the local velocity
v	rod lateral component of the local velocity
u_1	mixing vane tangential component of the local velocity
v_1	mixing vane normal component of the local velocity
F_u	axial component of the force exerted by the rod surface
F_v	lateral component of the force exerted by the rod surface
F_{u1}	tangential component of the force exerted by the mixing vane
F_{v1}	normal component of the force exerted by the mixing vane
F_A	total axial force
F_L	total lateral force
A	the flow area of the subchannel
A''_W	total wetted solid surface area of the subchannel including the mixing vane
A_R	wetted solid surface area of the subchannel excluding the mixing vane
A_W	mixing vane's wetted solid surface area
A_g	the gap flow area without mixing vane
A_{mg}	the gap flow area with mixing vane
D''_V	equivalent hydraulic diameter including the mixing vane
D_V	equivalent hydraulic diameter without the mixing vane
u_g	crossflow velocity across the gap
P	rod-to-rod pitch
S	gap width
z	axial height
D_h	hydraulic diameter of the 5x5 rod bundle
$W(i, j)$	crossflow between subchannel i and subchannel j

REFERENCES

1. D.S. Rowe. COBRA IIIC: digital computer program for steady state and transient thermal-hydraulic analysis of rod bundle nuclear fuel elements. Battelle Pacific Northwest Labs., Richland, Wash.(USA), 1973.
2. M. Glück. Validation of the sub-channel code F-COBRA-TF: Part I. Recalculation of single-phase and two-phase pressure loss measurements. Nuclear Engineering and Design, 2008, 238(9): 2308-2316.
3. H. Ninokata, A. Efthimiadis, N.E. Todreas. Distributed resistance modeling of wire-wrapped rod bundles. Nuclear Engineering and Design, 1987, 104(1): 93-102.
4. K. Rehme. Simple method of predicting friction factors of turbulent flow in non-circular channels. International Journal of Heat and Mass Transfer, 1973, 16(5): 933-950.
5. K. Rehme. Pressure drop correlations for fuel element spacers. Nuclear Technology, 1973, 17(1): 15-23.

6. A.Y. Gunter, W.A. Shaw. A general correlation of friction factors for various types of surfaces in cross flow. Trans. ASME, 1945, 67(8): 643-660.
7. M.A. Navarro, A.C.C. Santos. Numerical evaluation of flow through a 5X5 PWR rod bundle: effect of the vane arrangement in a spacer grid. International Nuclear Atlantic Conference, 2009, ISBN: 978-85-99141-03-8.
8. Y.F. Shen, Z.D. Cao, Q.G. Lu. An investigation of crossflow mixing effect caused by grid spacer with mixing blades in a rod bundle. Nuclear Engineering and Design, 1991, 125(2): 111-119.
9. E.E. Dominguez-Ontiveros, Y.A. Hassan. Non-intrusive experimental investigation of flow behavior inside a 5× 5 rod bundle with spacer grids using PIV and MIR. Nuclear Engineering and Design, 2009, 239(5): 888-898.
10. H.L. McClusky, M.V. Holloway, T.A. Conover, et al. Mapping of the lateral flow field in typical subchannels of a support grid with vanes. Journal of fluids engineering, 2003, 125(6): 987-996.
11. E.E. Dominguez-Ontiveros, Y.A. Hassan, M.E. Conner, et al. Experimental benchmark data for PWR rod bundle with spacer-grids. Nuclear Engineering and Design, 2012, 253: 396-405.
12. M.E. Conner, Y.A. Hassan, E.E. Dominguez-Ontiveros. Hydraulic benchmark data for PWR mixing vane grid. Nuclear Engineering and Design, 2013, 264: 97-102.
13. M. Avramova. Development of an innovative spacer grid model utilizing computational fluid dynamics within a subchannel analysis tool. The Pennsylvania State University, 2007.